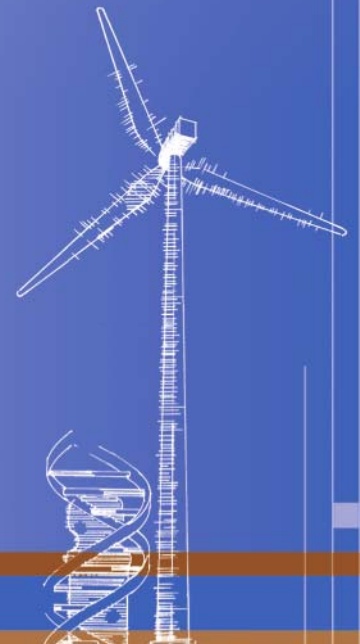# Comparing Pulsed Doppler LIDAR with SODAR and Direct Measurements for Wind Assessment

N.D. Kelley, B.J. Jonkman, and G.N. Scott
National Renewable Energy Laboratory

Yelena L. Pichugina
University of Colorado at Boulder

NOTICE

Available electronically at http://www.osti.gov/bridge

Available for a processing fee to U.S. Department of Energy
and its contractors, in paper, from:
>U.S. Department of Energy
>Office of Scientific and Technical Information
>P.O. Box 62
>Oak Ridge, TN 37831-0062
>phone: 865.576.8401
>fax: 865.576.5728
>email: mailto:reports@adonis.osti.gov

Available for sale to the public, in paper, from:
>U.S. Department of Commerce
>National Technical Information Service
>5285 Port Royal Road
>Springfield, VA 22161
>phone: 800.553.6847
>fax: 703.605.6900
>email: orders@ntis.fedworld.gov
>online ordering: http://www.ntis.gov/ordering.htm

Printed on paper containing at least 50% wastepaper, including 20% postconsumer waste

Comparing Pulsed Doppler LIDAR with SODAR and Direct Measurements for Wind Assessment

Neil D. Kelley, Bonnie J. Jonkman, and George N. Scott
National Wind Technology Center
National Renewable Energy Laboratory
Golden, Colorado 80401

Yelena L. Pichugina
Cooperative Institute for Research in Environmental Sciences/NOAA
University of Colorado at Boulder
Boulder, Colorado 80309

Abstract

There is a pressing need for good wind speed measurements at greater and greater heights to assess the availability of the resource in terms of power production and to identify any frequently occurring atmospheric structural characteristics that may create turbulence that impacts the operational reliability and lifetime of wind turbines and their components. In this paper, we summarize our results of a short study that compares the relative accuracies of wind speeds derived from a high-resolution pulsed Doppler LIDAR operated by the National Oceanic and Atmospheric Administration (NOAA) and a mid-range Doppler SODAR with wind speeds measured by four levels of tower-based sonic anemometry up to a height of 116 m. The level of accuracy to which the inter-comparisons with the LIDAR and SODAR could be compared with the sonic anemometers is limited by the degree of local flow distortion as a result of the presence of the tower and the nature of obstructions locally mounted near each anemometer. We performed an optimized inter-comparison between the LIDAR and sonic anemometers which agrees quite well with an earlier and similar study that used a predecessor of the current NOAA LIDAR. Finally, we summarize the results of inter-comparing a relatively long-term and generally non-contiguous record of horizontal wind speeds measured simultaneously by the SODAR and the four sonic anemometers.

Introduction

As part of a cooperative program between GE Energy and the National Wind Technology Center (NWTC), a two week experiment was conducted in conjunction with the Environmental Technology Laboratory (now the Earth System Research Laboratory or ESRL) of the National Oceanic and Atmospheric Administration (NOAA) on the High Plains south of Lamar, Colorado. This experiment concluded the more extensive Lamar Low-Level Jet Project [1, 2] that took place from October 2001 through September 2003. The purpose of this study was to characterize the vertical wind shear and turbulence characteristics associated with Great Plains Nocturnal Low-Level Jet Streams and use that information to develop turbulent inflow simulation models. During this two week experimental period the NOAA High-resolution Doppler LIDAR (HRDL) was used simultaneously with measurements from a mid-range Doppler SODAR and a 120-m meteorological tower to measure the dynamics of the wind fields in close proximity. Since the primary objective of this experiment was to characterize the turbulent structures associated with the low-level jet, the dominant LIDAR scanning mode employed was not optimized for inter-comparing the horizontal wind speeds measured by the SODAR and tower-mounted sonic anemometers. However, we did utilize one LIDAR scanning mode that was specifically optimized for directly comparing the 3-D wind vector measured by the sonic anemometers and aligned with the corresponding LIDAR radial wind speed. We took advantage of a much longer LIDAR record that used a vertical scanning technique to derive a mean vertical wind speed profile and then compared it with
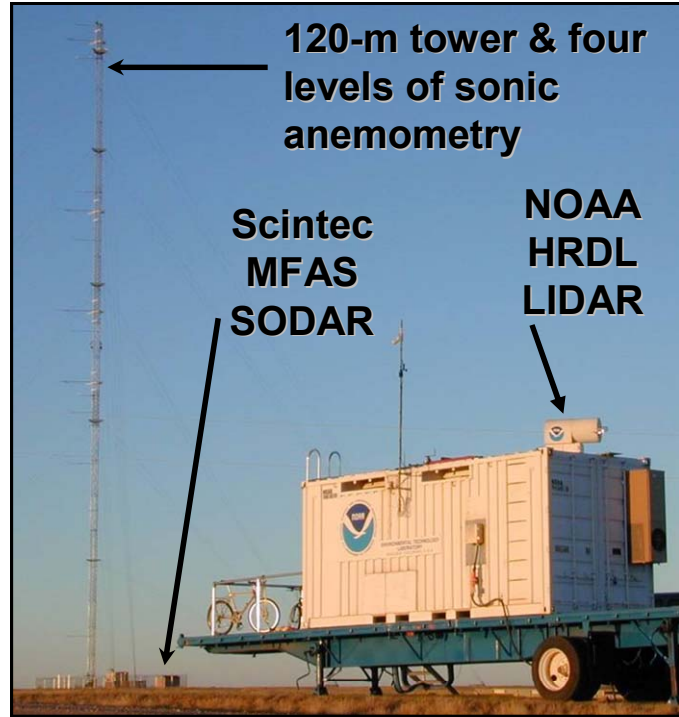
simultaneous measurements from the SODAR and sonic anemometers. In this paper we discuss the details and results of this unique opportunity to inter-compare two remotely sensed wind finding technologies with simultaneous in-situ measurements.

The Observing Systems

Three measuring systems were used for this inter-comparison: (1) three-axis sonic anemometers mounted at four heights on a 120-m meteorological tower, (2) a mid-range SODAR that was programmed to operate over a range of 50 to 500 m above ground level (AGL), and (3) a pulsed Doppler LIDAR with a nominal operating range of 0.2 to 3 km and 30-m resolution along its scanning beam. The photo in Figure 1 depicts the relative positions of these three systems with their plan position locations shown schematically in Figure 2.

The Meteorological Tower and Sonic Anemometers

Sonic anemometers were installed at heights of 54, 67, 85, and 116 m AGL on a 120-m triangular lattice tower whose side dimensions are 1 to 1.2 m wide depending on height. The tower is specifically designed to be torsionally very stiff in order to minimize angular twisting motions in high winds that could induce false velocity readings in the sonic anemometers mounted on instrument arms some distance from the main tower structure. Devices called "star" mounts were employed to connect dual guy cables in such a way as to provide increased torsional resistance. The sonic anemometers were mounted a minimum distance of nearly five tower widths (~ 5 m) from the tower structural envelope on instrument arms that are specifically designed to appreciably damp out arm

Figure 1. Physical arrangement of the SODAR and LIDAR with respect to the 120-m tower on the Emick Ranch (Colorado Green Wind Farm) south of Lamar, CO.
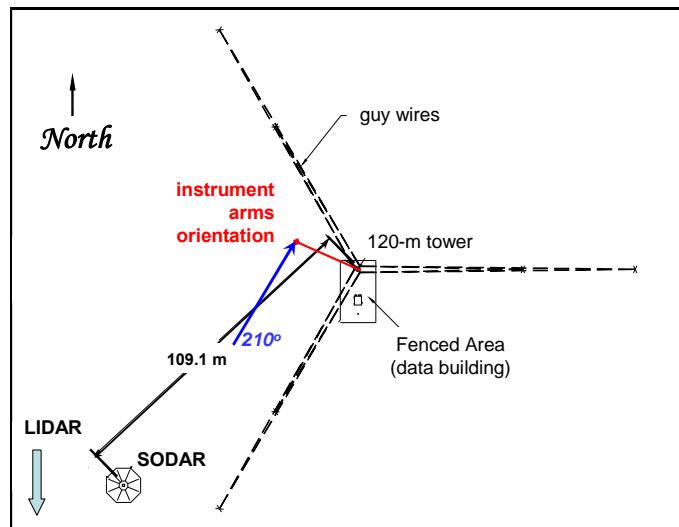
Figure 2. Plan positions of the SODAR and tower and the orientation of the instrument support arms and wind direction used for the optimal LIDAR-Sonics inter-comparison.

vibrationally-induced motions occurring within the desired velocity measurement frequency range of 0 to 7 Hz. The arms were aligned towards 300° with respect to true north. The reference anemometers are Applied Technologies Inc. Model SAT/3K (Kaimal design) three-axis sonic anemometers whose three

component velocities are available with a time resolution of 0.05 s and a 7 Hz bandwidth. The anemometers have a 15 cm path length and provide a velocity resolution of 0.01 m/s with the manufacturer's claimed accuracy of ±0.05 m/s.

The Mid-Range SODAR

A Scintec Model MFAS mid-range SODAR shown in Figure 3 has a vertical resolution of 10 m and was operated over a nominal height range of 50 to 500 m AGL. The horizontal velocity resolution was ~ 0.4 m/s with an expected accuracy of ±0.3 m/s or better. The instrument incorporates a 64 element phased array antenna and provides a maximum acoustic output power of 7.5 W. The antenna was placed within a custom-built support frame on the ground in the center of a free standing acoustic enclosure (see Figure 3). The frame provided a leveling accuracy of the antenna to better than one arc second. The antenna was positioned 109.1 m southwest of the tower center so that the primary antenna radiation lobes would not illuminate the tower (see Figure 2). This placement minimized the spatial separation between the SODAR measurement volumes and the tower instrumentation which improved the observed correlation of the horizontal wind vectors derived from each source.

In order to take full advantage of the capabilities of the Scintec signal processing software, the SODAR was operated (during the LIDAR-SODAR-Tower inter-comparison period reported on in this paper) in a multi-beam and multi-frequency mode. Pulse sequences from one vertical and eight tilted beams were radiated in the following sequence of Vertical, East, North, Vertical, South, and then West. The horizontal wind speeds and directions are derived from the primary or cardinal direction (East-North-South-West) pulse beams that are tilted 29º from the zenith and illustrated schematically in Figure 4. As a pulse in each cardinal direction is radiated, a complimentary pulse inclined 22º from the vertical is radiated towards the opposite direction but for clarity are not shown in Figure 4. For each primary beam direction a sequence of ten pulses whose frequencies ranged from 1816.4 to 2741.7 Hz with corresponding pulse lengths varying from 30 to 70 m were emitted in an attempt to improve
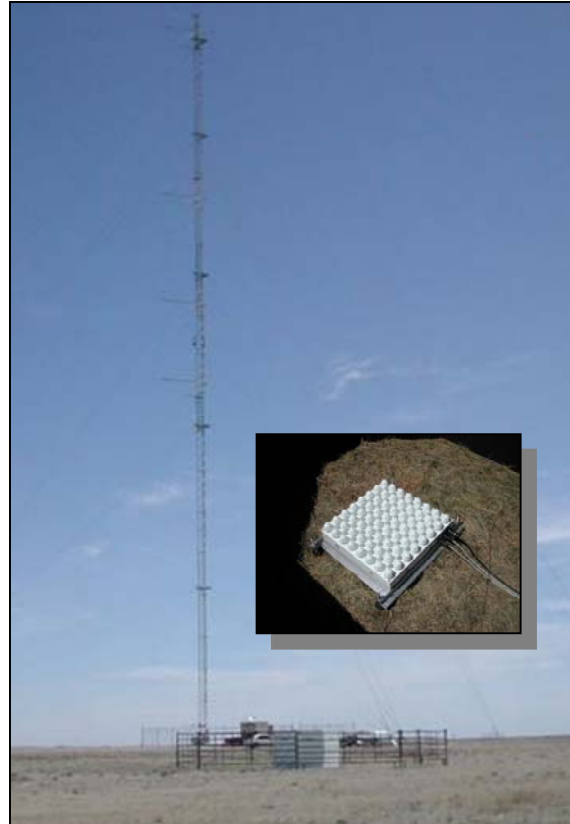
Figure 3. Scintec MFAS SODAR and 120-m tower with antenna installed within acoustic enclosure (insert).
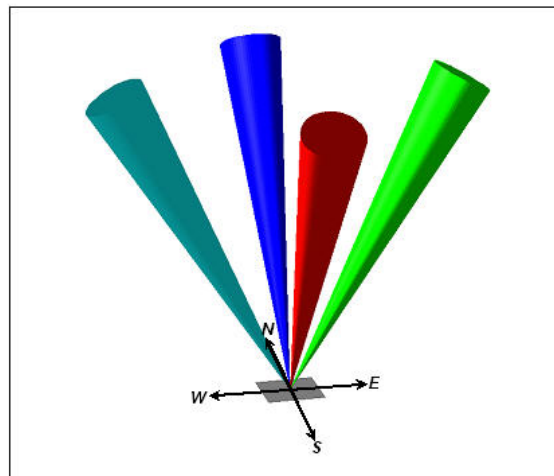
Figure 4. Schematic of the primary SODAR beams that are tilted 29º from the zenith. The 22º complimentary and vertical beams are not shown for clarity.

3

the backscattered signal-to-noise ratio (SNR). The integration or averaging time used was 20 minutes, but results were recorded at 10-minute intervals. The site was acoustically very quiet (or at least very quiet within the operating frequency range of the SODAR) which allowed the automated receiver to achieve very high sensitivities at large ranges (heights) which improved the SNR and subsequently the horizontal wind vector measurement performance. Because a phased array antenna radiates a high number of secondary or side lobes in addition to the primary one, the energy in some of these lobes illuminated the 120-m tower and was reflected back to the antenna. This situation presents a number of fixed echoes to the SODAR. While there is no Doppler frequency shift and therefore no wind velocities associated with such echoes, they can mask or overwhelm the often weaker velocity-related return signals. The use of multiple frequencies often helped in this regard, and when coupled with the Scintec signal processing software, did an excellent job of detecting and ignoring these fixed echoes from the tower and improving the wind speed measurements. Poor SODAR performance often occurs late in the afternoon when the atmosphere is thermally well mixed. It also can be very poor when the relative humidity in the height layer through which the SODAR is measuring decreases to less than 40% as a result of the increased atmospheric absorption of the radiated and backscattered acoustic energy. This occurs frequently due to the high plains location of the Lamar Site and often limits the usefulness of the SODAR. This was particularly true during the summer of 2002 when the region was under a severe drought.

Wind Finding LIDAR

While Doppler SODARs measure the wind from *acoustic energy* that is backscattered from small-scale turbulent fluctuations of temperature (density), Doppler LIDARs use the *light energy* backscattered from microscopic particulates or aerosols being transported by the wind. The very high sensitivity of modern electronic amplifiers has allowed a modern LIDAR like the HRDL to measure wind fields out to ranges of several kilometers even when the air is quite clean and contains low numbers of usable scattering particles that result in very low backscattered signal levels. The need for atmospheric LIDAR to meet be eye safety standards limits the both the intensity of the light energy and its highest frequency (shortest wavelength) that can be focused and radiated. When these criteria are combined, LIDARs used for atmospheric measurements use mid-range infrared light generated by lasers operating with wavelengths in the 1.5 to 2 μm range. The peak radiated power depends on the wavelength and whether or not the LIDAR is being operated in a pulsed or continuous mode. The peak power used with most LIDARs is typically less than 2 mJ.

Atmospheric wind-finding LIDARs come in two general forms: continuous wave (CW) or pulsed. A CW LIDAR uses the continuous emission of light energy through optics that focuses the beam over a certain radial distance ahead of the instrument. It is within this focus region that backscattered energy is collected and the relative motion of the field of targets determined from the Doppler frequency shift. Often the signal representing this velocity is initially sampled at very high rates and then significant smoothing is applied to reduce the variability to improve the SNR and ultimately the accuracy of the derived wind speed. In order to measure the wind speed at other locations, the focus region must be relocated and/or the elevation angle of the radiated beam varied.   CW wind finding LIDARs typically perform a *conical scan* sequence in which one or more 360º scans are performed at a fixed elevation angle and focus position. The process is repeated with the focus repositioned at other ranges. Some CW LIDARs vary both the focus and the elevation angle in a more complex scanning sequence. After the scanning sequence has been completed, a Velocity Azimuth Diagram or VAD is calculated to locate the magnitude and azimuth of the peak wind speeds at the height associated with the elevation angle and radial distance of the center of the focus region. The results from the scans at the various focus ranges and perhaps multiple elevation angles are then combined to form the resulting wind profile. CW LIDARs typically only produce measurements of the mean horizontal wind vector at a few heights but with very good accuracy when optimal smoothing is applied.

Pulsed LIDARs, as their name implies, emit regularly spaced emissions of highly collimated light energy for a specified period of time (pulse length) similar to a Doppler SODAR. Precision timing circuits then isolate the returned signals to a period of time that corresponds to a specified segment of radial distance along the beam called a *range gate*. The backscattered signals contained within each gate are then processed to derive the line-of-sight (LOS) or radial velocities along the path of the LIDAR beam. Pulsed LIDARs typically operate with pulse repetition or sampling frequencies ranging from 200 to 1,000 pulses (samples) per second. Smoothing is applied that provides typical time resolutions of 0.1 to 0.5 s in the derived velocities. The advantage of the pulsed LIDAR is the ability to resolve a 3-D flowfield through the application of various scanning sequences, including the conical scan discussed above. The resulting vertical wind profile derived from a pulsed LIDAR using a conical scan incorporates a much greater vertical resolution than an equivalent CW profile. The fineness of this resolution is a function of the width of the range gates and the elevation angle used.

The NOAA HRDL Research LIDAR

The HRDL uses a Tm:Lu, YAG solid state laser operating a wavelength of 2.0218 μm. For this experiment the LIDAR was configured to be pulsed at 200 per second with energy of 1.5 mJ and a radial range (gate) resolution of 30 m. The minimum range was 0.189 km and the nominal usable maximum range was ~ 3 km.   The collimated beam diameter ranged from 0.06 to 0.28 m (at 3 km). The measured radial velocities could be resolved to ~ 0.1 m/s in speed and 0.25 s in time. The design details of the HRDL and its uses are discussed by Grund, Banta, et al [3].

The primary scanning mode used for this experiment was the vertical sector scan. Here the azimuth angle is aligned pointing into or with the mean wind direction and remains constant while the elevation sweeps through a desired angle range and rate.   This mode provides a vertical slice of the wind field parallel to the mean wind. An example of this type of scan display is shown in Figure 5. This display allowed us to identify in real time the presence of low-level jet streams and associated flow features such as atmospheric wave motions that have been shown to be important to wind turbines [4]. This mode was also used to inter-compare the wind profiles derived from the SODAR with the HRDL and will be discussed more fully later in this paper. Periodically a short-duration conical scan was performed to (1) assess the horizontal extent of atmospheric wave motions seen in the vertical scan and exemplified in Figure 6, and (2) to obtain a vertical wind profile associated with the presence of those wave structures such as that depicted in Figure 7.

We employed a "stare" mode in which both the azimuth and elevation angles remained fixed for two specific purposes.
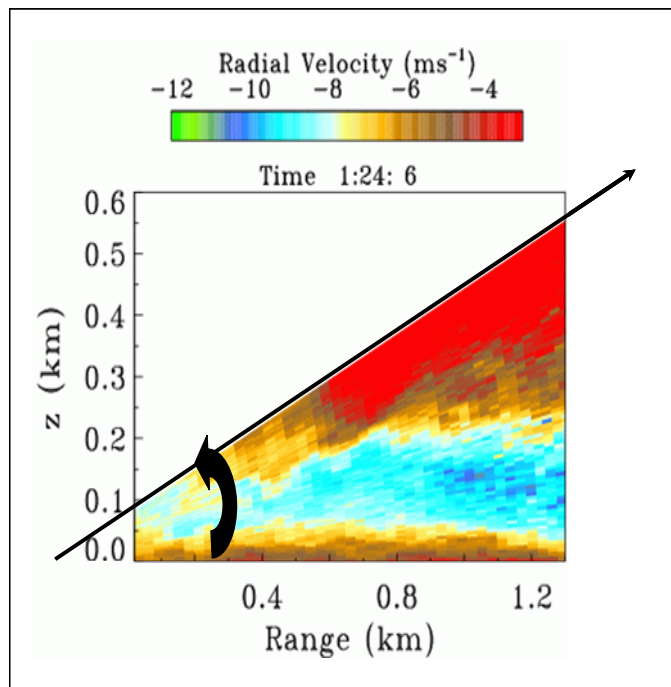

Figure 5. An example of a LIDAR vertical scan while at a fixed azimuth angle. The observed radial wind speed is indicated by the color code and shows the presence of a low-level jet stream (cyan & blue) at a height of about 0.125 km with a peak wind speed of 10-11 m/s. The negative wind speeds indicate that the wind is blowing towards the LIDAR.

5

In the first we positioned the HRDL beam to be near the sonic anemometer at either the 85-m or 116-m tower levels in order to perform an inter-comparison of the velocities measured by each of the instruments. We will discuss the details of this application later in the paper. In the second we aligned the beam parallel with the mean wind direction at an elevation angle of 10º when the vertical scan mode had indicated the presence of organized structures in the wind field. This scan mode allows a vertical wind profile to be generated with a 5-m vertical resolution from 35 to 233 AGL using the velocities derived from each of the range gates out to a range of about 1 km. By removing a 5-minute running mean from the velocity measured in each range gate with a low-pass filter we can obtain a picture of the spatial structure organized motions of turbulent kinetic energy (TKE) from the LIDAR and compare them with the corresponding in-situ measurements from the sonic anemometers on the tower as demonstrated in Figure 8.

## Estimates of Local Flow Distortion near Tower-Mounted Sonic Anemometers

We began by inter-comparing the horizontal wind speeds and directions from the SODAR and tower-based sonic measurements because the largest record (~ 585 hours) is available from these instruments. It became clear early that while the population mean and median differences or biases from all four
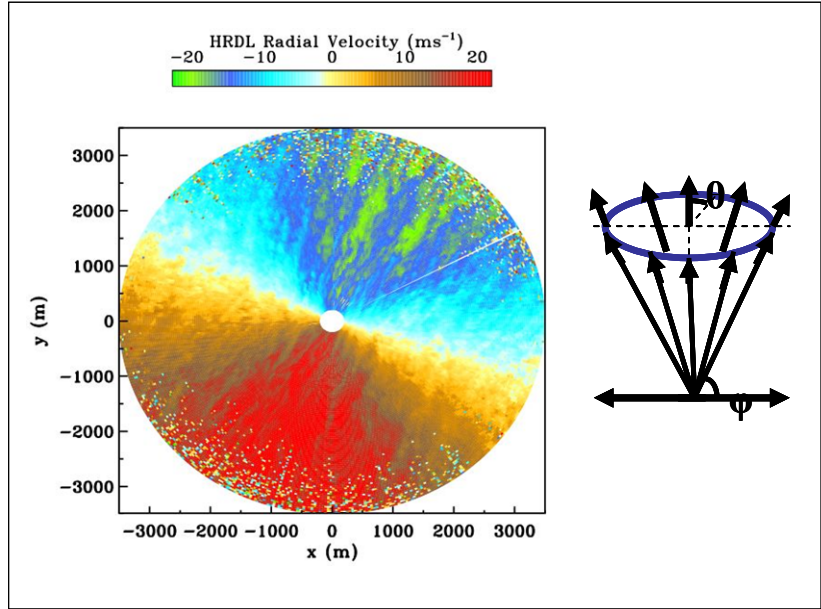
Figure 6. An example of a plan view of a HRDL conical scan at a fixed elevation angle and shown schematically at the right. Positive velocity values (red) indicate the wind is blowing away from the LIDAR and negative (blue) values indicate it is blowing towards it. The bright green areas in the upper right quadrant indicate organized regions of higher speed and turbulent air.
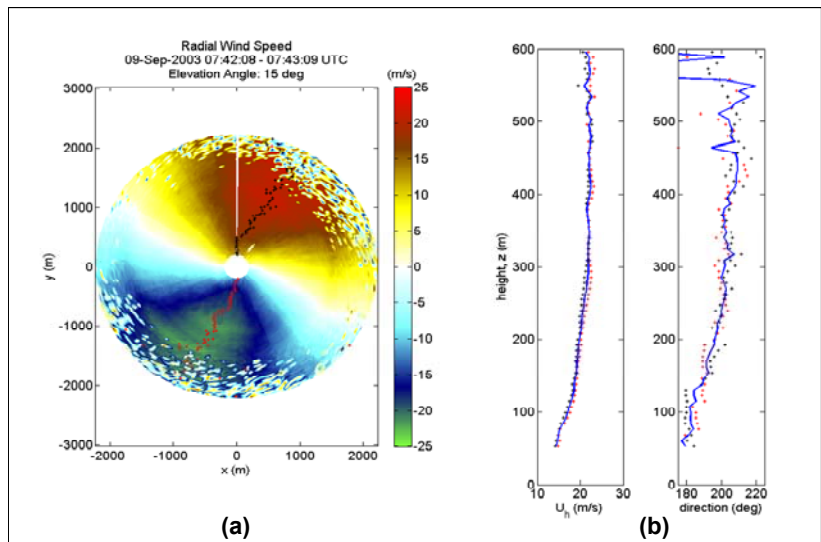
Figure 7. Example of a LIDAR 360º conical scan showing: (a) the plan view with the radial wind speed color-coded; (b) the corresponding 8-m vertical resolution profiles of the horizontal wind speed U_H (left) and the wind direction (right). The dots at each resolved height indicate the observed range of the variables.
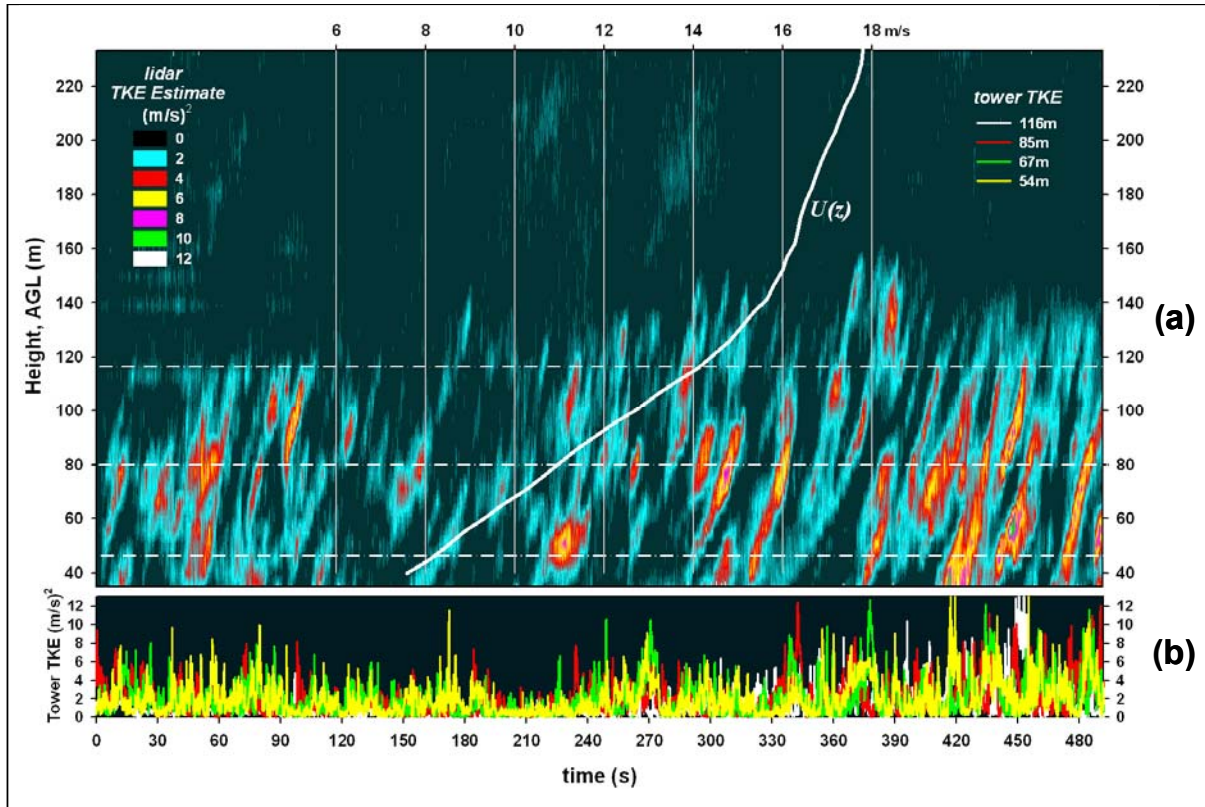
Figure 8. Example of a comparison of the time variation of the vertical distribution of turbulent kinetic energy (TKE) estimated from: (a) LIDAR fixed azimuth and 10º elevation angles stare scan; (b) directly from the four tower-mounted sonic anemometers. The mean horizontal wind speed profile, U(z), is also shown and scaled at the top of the diagram. The horizontal dashed lines represent the lower limit, the hub, and the upper limit heights of a GE 1.5 MW wind turbine.

measurement heights were small (+0.13 and -0.06 m/s respectively for the horizontal wind speed and -3.4 and -3.2 degrees respectively for the wind direction), the biases and slopes (ratios) were a function of height. This can be seen in Figure 9 in which the variation of the mean bias or offset and slope (ratio) of the horizontal mean wind speed UH from the SODAR and sonic anemometers are plotted as functions of height. Restricting the analysis to observations in which the SODAR received SNR was high or very high made some improvement, but it was obvious that the bias becomes increasingly negative with increasing height while the slope does just the opposite. The wind direction mean bias ΔWD (where WD is the wind direction in degrees from each of the instruments) also increased with height but there was no definitive trend in the height variation of the slope suggesting that the local flow conditions at each sonic anemometer location were somewhat unique. A further examination of the data revealed that the U_H and WD slopes and biases varied with not only height but with the wind direction or approach angle.

The close proximity of the SODAR to the tower and limiting the comparisons to observations in which the SODAR return signal exhibited a high or very high SNR allowed us to prepare a 2-D mapping of the wind speed and direction biases (the SODAR value subtracted from the sonic) as functions of the mean wind direction (approach angle) and speed for each sonic anemometer height. The results are shown in Figure 10 for the angular range of 140 degrees clockwise through north (360°) to 100 degrees ignoring the azimuth sector from 100 to 140º because the flow was coming through the tower structure. We have

indicated the azimuth toward which the instrument support arms were aligned (300º). The wind speed bias clearly is positive (the sonics reading higher than the SODAR) at wind speeds below about 10-11 m/s but becomes negative for higher wind speeds at most wind directions. This suggests a strong wind speed dependence that we believe is related to the cylindrical members that form the lattice structure of the tower. The large, vertical apex legs of the triangular tower have a diameter of 8.9 cm from the base up to about the 60-m level and then 7.6 cm from there to the top. The lattice cross members have a diameter of 3.8 cm.
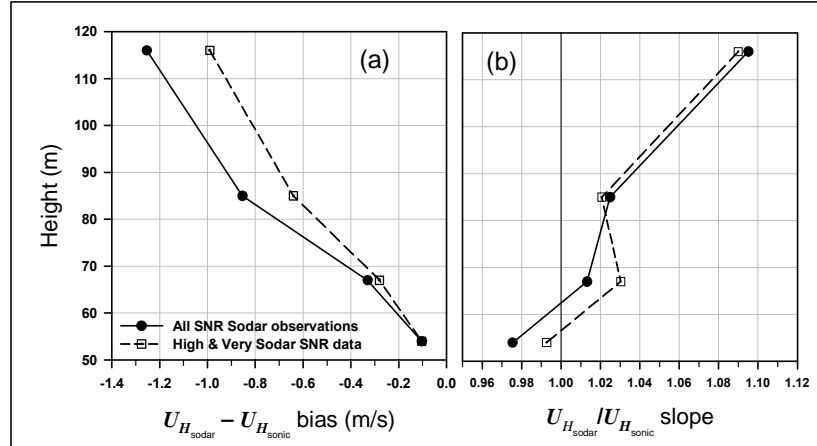
Figure 9. The observed height variation in the linear regression results of the UH measured by the SODAR referenced to the sonic anemometers: (a) the bias (offset); (b) the ratio of the slope of the UHsodar referenced to the UHsonic. Wind speeds derived from SODAR measurements at all non-zero SNRs are shown with a solid line and filled circle and those with high and very SNRs are shown with a dashed line and dotted square.

The Effects of the Tower Cylindrical Structural Elements

We previously demonstrated in [2] that the tower lattice cross members were responsible for Aeolian vortex shedding at a wind speeds near 10 m/s that excited a narrowband vibration in the sonic anemometers. This vibration induced an 8.5 Hz spike in the recorded velocity signals. The strong dependence of the observed sonic wind speed bias relative to the SODAR (positive below about 10 m/s and then negative above) with the corresponding SODAR mean wind speed suggested a change in the drag that influenced the local flow characteristics around the individual cylindrical structural elements that produces an integrated flow effect beyond the tower structural envelope. Figure 11 shows the variation of the drag coefficient C_D versus Reynolds number (Re) for the flow perpendicular to the long axis of a cylinder (cross flow) derived from fitting the data of Weiselsberger [5] and Achenbach [7]. For a Re range of about 20,000 to 200,000 the value of C_D remains essentially constant but then drops very rapidly, reaching a minimum in the vicinity of about 430,000 before beginning a slow increase. Figure 12 places the best-fit C_D versus Re relationship in Figure 11 into perspective for the three cylindrical structural element diameters over the equivalent range of observed SODAR high SNR mean wind speeds. The rate in which the drag coefficient is changing on the three cylinder diameters ($\Delta C_D/\Delta U_H$) over this wind speed range is plotted against the right axis in Figures 13a and 13b with the corresponding mean wind speed (ΔU_H) and direction biases (ΔWD) of the sonic anemometers relative to the SODAR referenced to the left axis. Below 10 m/s where the drag is high and its rate of change is decreasing, we note that ΔU_H is also decreasing with increasing wind speed and changes sign between 10 and 11 m/s. In Figure 13b the corresponding wind direction bias ΔWD increases with decreasing drag until a speed of about 12.5 m/s is reached and then becomes nearly constant as the drag reaches its minimum and begins to slowly increase again. Clearly the character of the flow field around the tower is being significantly influenced by this rapid decrease in drag with increasing wind speed seen by the tower cylindrical structural elements. We believe this is basis for the strong correlation in the observed variation in ΔU_H between the sonics and SODAR shown in Figures 9 and 10. The number and density of the cross members incorporated into this tower design in order to provide the desired torsional stiffness has resulted

8

in a relatively high porosity (blockage) that varies only slightly with wind speed and has undoubtedly contributed to the observed magnitudes and sensitivity of the speed and direction biases with wind speed even as far away as five tower widths.
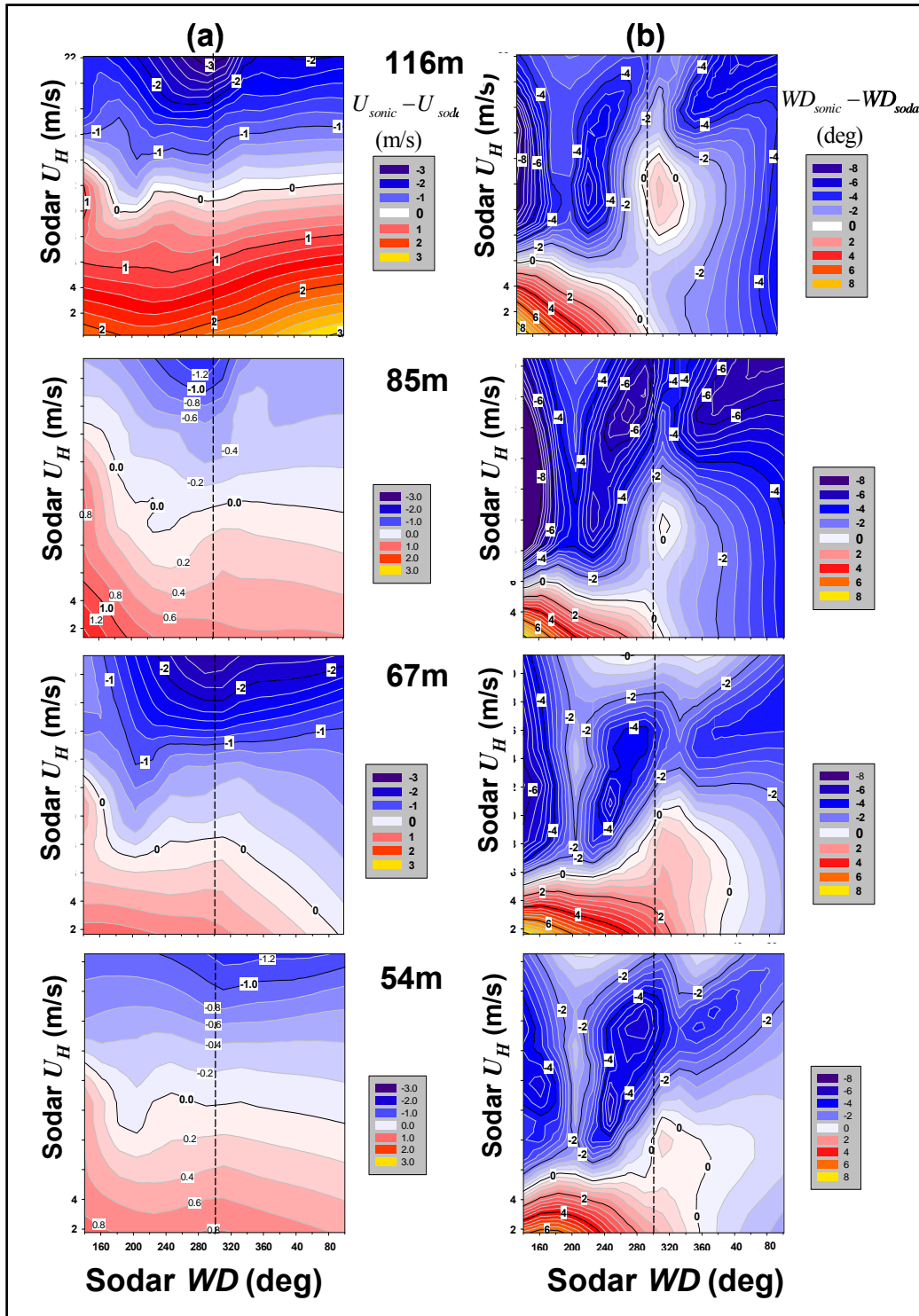

Figure 10. Observed variation in the observed difference in the SODAR and sonic anemometer wind vector with height: (a) wind speed; (b) wind direction. The orientation of the instrument support arms are shown with a dashed line.
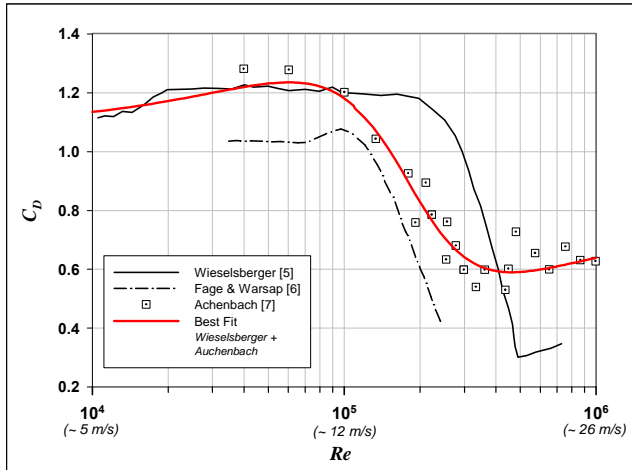
Figure 11. Variation of cylinder drag coefficient, C_D, with Reynolds number, Re, (based on cylinder diameter).
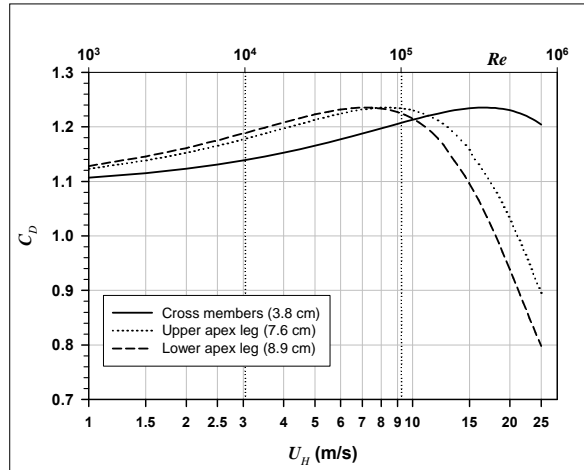

Figure 12. Variation of C_D with wind speed using the best fit C_D vs Re curve of Figure 11 for the three cylindrical structural elements of the Lamar Tower.

The Variation of Speed and Direction Biases with Flow Approach Angle

A detailed view of the tower and the equipment mounted on it are shown in Figure 14. The variation of ΔWD with the wind approach angle (SODAR WD) pictured in Figure 10 shows much more detail than the corresponding variation of ΔU_H. Some of the features are similarly repeated at each height such as the contours of high ΔWD and low ΔWD bias respectively to the left and right of the instrument arms when the flow approaches from 240 and 320 degrees in the neighborhood of 10 m/s. The relative magnitudes of the biases vary with height with the 67- and 116-m levels demonstrating the largest variations. We believe this to be the result of the amount of equipment mounted on the tower near these levels. For example, there is a shorter instrument arm mounted just below the sonic at the 67-m height, and the mid-tower aircraft warning beacons are located in the same vicinity. At the 116-m level, two shorter instrument support arms, a convergence of guy cables connecting to a "star" mount, and the upper aircraft warning beacons all serve to distort the nearby local flow regime in addition to the instrument arm that the sonic itself is mounted on. Figure 10 demonstrates just how difficult it is to achieve accurate wind flow measurements on lattice towers when both measurement and operational requirements must be considered. The end result is that the tower-based
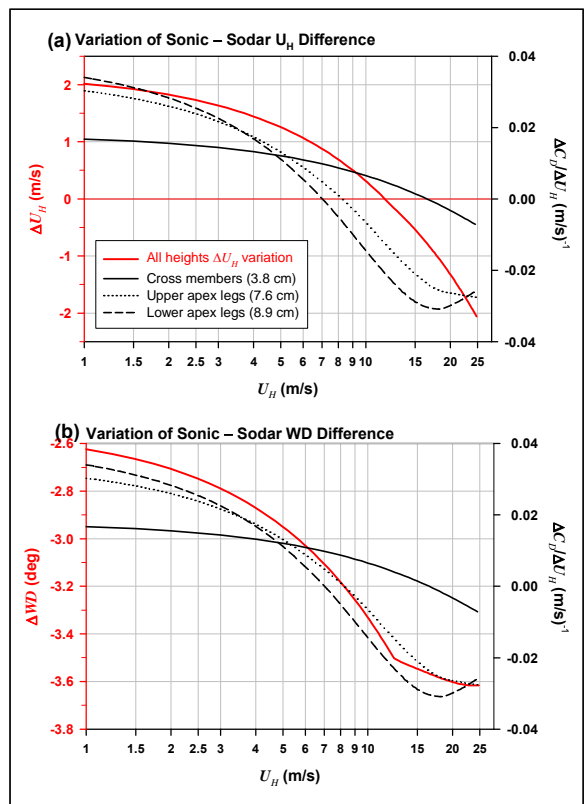

Figure 13. Rate of change in differences of horizontal wind speed (U_H) and direction (WD) between SODAR and sonic anemometers versus rate of change of C_D with wind speed, $\Delta C_D/\Delta U$: (a) ΔU_H ; (b) ΔWD using best fit C_D vs Re curve of Figure 11.
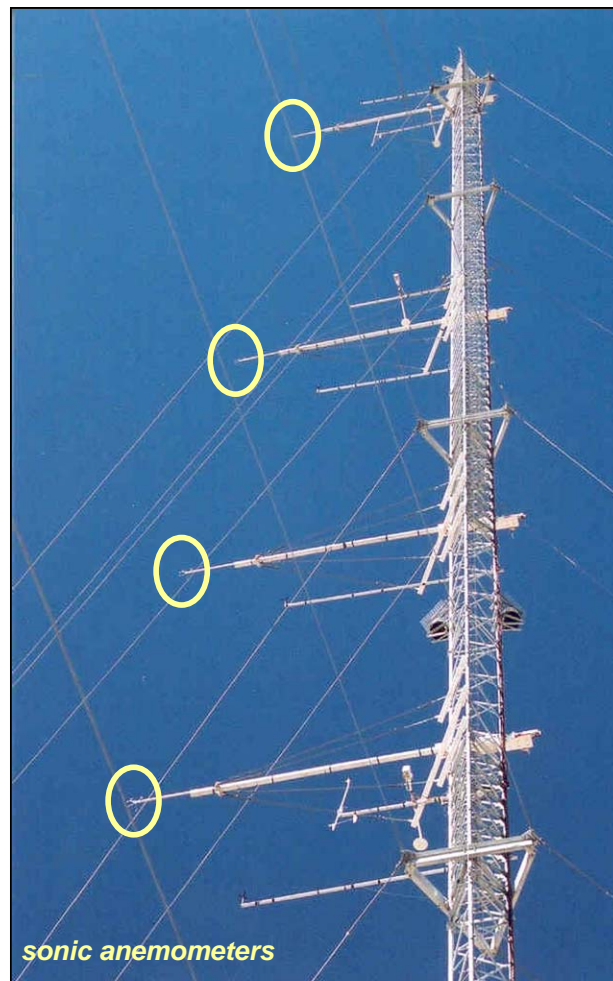
10

measurements made from instruments mounted on support arms cannot be considered the ultimate reference when comparing wind speeds simultaneously derived from SODAR or LIDAR measurements, but they can be used to achieve a consensus of the wind field. If a comparison of the underlying accuracy of a remote sensing device with a direct measurement is desired, the use of a precision sonic anemometer (15-bit resolution and known flow distortion profile) installed atop a stiff cylindrical tube attached to a lattice tower base is probably the only recourse.

LIDAR Wind Field Measurements

The nature of the Lamar experiment relied heavily on the fixed azimuth, vertical scanning mode of data collection with the HRDL. As a result, the majority of the data available for inter-comparison with the SODAR and tower sonic anemometers had to come from this data collection mode. Periodically the HRDL was placed into a conical scanning or VAD mode (one or two fixed elevation angles each with a complete 360º rotation in azimuth) but the total record length generally was the order of one or two minutes and insufficient for an adequate inter-comparison with the 10-minute mean values derived from the SODAR and sonic anemometers. As previously mentioned, we did employ one dedicated HRDL scan mode to inter-compare the LIDAR radial velocities with the equivalent velocities derived from the 85- and 116-m level sonic anemometers. However, there are only a limited number of short records available due to the highly restrictive requirements; i.e., a very narrow range of acceptable wind directions relative to the orientation of the sonic anemometers and their support arms.

sonic anemometers

Figure 14. A close-up view of the sonic anemometers, their mounting arms, and nearby instrumentation and tower support apparatus.

Wind Speed Profiles Derived from the LIDAR Vertical Scan Mode

Wind speed profiles were derived from the LIDAR vertical scans by first applying quality control procedures to the radial velocities in each range gate, such as insuring that there were no fixed echoes present and that the SNR of the returned signal was sufficient to obtain a good velocity measurement. The horizontal wind component U_H was derived by dividing the measured radial velocities in each range gate by the cosine of the associated elevation angle and sorted into 10-m vertical bins for each individual vertical-slice scan as shown schematically in Figures 15a and 15b. An average was calculated for each height bin over the length of the record (10 minutes). This technique allowed us to derive a vertical profile of U_H with the same heights and over the same time periods as the SODAR and sonic anemometers for direct comparisons. The limitations of this approach include the consequences of a lack of horizontal homogeneity at low elevation angles (large variations in the radial velocity over the

11

observed range), the sparse spatial sampling at high elevation angles, and the influence of the vertical wind component not being taken into account when deriving the values of U_H.

Fixed Stare Scanning Mode

In order to minimize the influence of the distorted flow around the tower and achieve the best measurements of the wind velocity vectors at each of the sonic anemometers, we chose a mean wind direction (210º) that aligned the flow perpendicular to the sonic and its instrument support arm. We then aligned the LIDAR beam parallel to this flow and moved it a small distance to the West of the sonic anemometers to avoid creating a fixed echo. These alignments are pictured schematically in Figures 16a and 16b. The radial velocities measured in Range Gates 6 and 7 were used for the inter-comparisons with the sonic anemometers. Noise spikes were removed from the LIDAR measurements before the two range gates were averaged to give radial velocities at the corresponding sonic anemometer heights. To account for wind direction, the quality-controlled total velocity vectors from the sonic anemometers were projected onto a vector aligned with the same azimuth and elevation angle as the LIDAR beam. The magnitude of the velocities from the LIDAR and the projected sonic anemometer were then inter-compared.
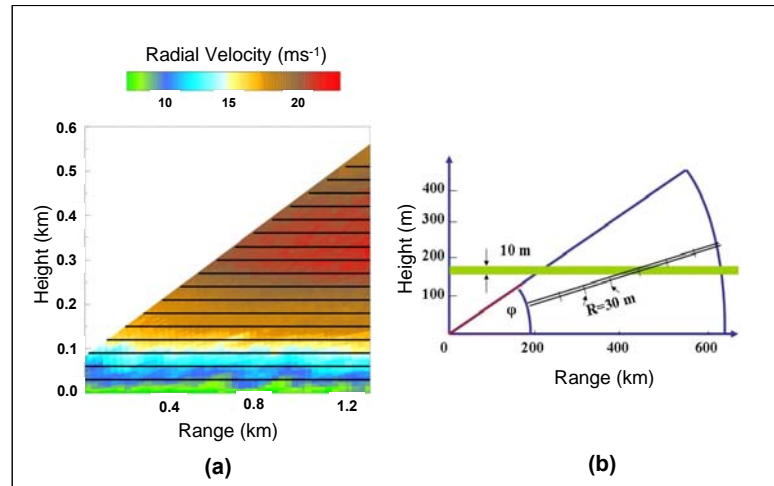
Figure 15. Example of LIDAR vertical sector scan mode display: (a) colors represent the radial wind speed component with the sector divided into 10-m vertical bins; (b) schematic of how the vertical-binning process is applied using the 30-m wide range gates.
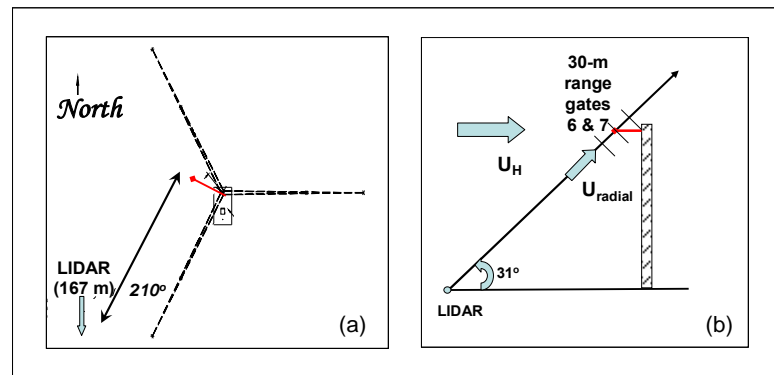
Figure 16. Alignment of LIDAR stare scan with respect to 120-m tower for optimized sonic anemometer inter-comparison: (a) plan view; (b) elevation view.

RESULTS

We used the period when the NOAA HRDL was available to formally inter-compare the simultaneous mean values of U_H measured with the:

1. tower sonic anemometers and the SODAR

2. tower sonic anemometers and the LIDAR derived from the vertical scanning mode

3. LIDAR from the vertical scanning mode and the SODAR.

We performed what we believe to be an optimum but relatively limited inter-comparison between the fundamental velocities measured by the LIDAR; i.e., the radial wind or LOS velocity component along the beam, and the total wind vector measured by a three-axis sonic anemometer and projected onto an equivalent radial vector component at the sonic anemometer measured in the neighborhood of the LIDAR beam. We also took advantage of the availability of long-term simultaneous measurements from the tower sonic anemometers and the SODAR collected over an aggregate period of 585 hours between the last week of May through mid November 2002 (excluding the month of October) and again for three weeks before and during the LIDAR measurement period in 2003.

Sampling Volume Considerations

It is important to note that the actual measuring volumes associated with each of the three measurement systems vary by several orders of magnitude and are likely a significant contributor to the observed levels of RMS uncertainty observed in the individual inter-comparison pairs. The sonic anemometers measure the three components of the wind vector (streamwise, crosswind, and vertical) along three separated orthogonal axes. The wind speed component parallel to each axis is measured by the time it takes (time-of-flight) for an ultrasonic (200 kHz) pulse to make the roundtrip over the path length of 15 cm. For our purposes here we consider, to a first approximation, that the sampling volume of the sonic anemometers is related to the physical separation of the three measurement paths within the spatial geometry of the sensing head (shown in Figure 17). We further assume that the wind vector is being sensed within a spherical volume whose diameter encompasses the physical extent of the three measurement arms shown in Figure 17. We have estimated this diameter to be 46 cm. This dimension allows us to arrive at an estimated measuring volume of 0.05 m^3 that we can use to compare with the two remote sensing systems at least on an order of magnitude basis.

The effective beam diameter of the HRDL for this experiment varied with range starting at 8 cm at the minimum range of 0.2 km, decreases to 6 cm at 800 m, and then increases again at an approximately linearly rate to 28 cm at the typical maximum usable range of 3 km [8]. The average beam diameter for Range Gates 6 and 7 used with the stationary, fixed stare scanning measurement is 7 cm for a mean physical measuring volume of 0.23 m^3 (assuming that the backscattered signal contributions remain within the physical distance of 60 m for the combined range gates). For estimating the value of U_H using the vertical scanning mode at low elevation angles, the measurement volume varies along the beam from 0.08 m^3 at the minimum range to 1.85 m^3 at the maximum range of 3 km.

The sampling volumes associated with the SODAR are bit more complicated. During this experiment the wind speed and directions were measured individually by eight tilted beams whose results were then combined into the final result. Depending on the SNR, the results could be based on the usable signal returns from as few as two beams to as many as eight. Further, the manufacturer's specifications do not list the effective beam width (width of the primary lobe) of this instrument which we need to estimate the sampling volumes. Based on the characteristics of similar acoustic phased array antennas and those used by other SODAR manufacturers we believe this value is in the neighborhood of 10 degrees (at least for comparative

Figure 17. ATI/Kaimal 3-axis sonic anemometer sensing head (*courtesy Applied Technologies, Inc.*)

purposes). The contents of Table 1 summarize the calculated sampling volumes, the separation distances to the center of the beams, and the diameter of the beams at the mid height of the associated range gates. We have also included the 200-m level AGL for completeness since that is the height that will likely be reached by future 10 MW turbines. The SODAR backscattered energy was collected from turbulent temperature structures within much larger volumes and therefore subjected to much greater spatial smoothing than the sonic anemometers and the LIDAR. Like the LIDAR when it was scanning at very low elevation angles, the SODAR was also collecting backscattered energy from sampling in the same vertical layer but separated horizontally. These spatial differences could be a contributor to the RMS variations in the observed differences in wind speed seen between the tower sonic anemometers and the LIDAR when highly inhomogeneous flows are present, such as during a stable boundary layer populated with breaking atmospheric wave motions.

Table 1. SODAR Sampling Volumes and Beam Separations at Sonic Heights

Height	Sampling Volume (m³)		Mid Gate Beam Diameter	Horizontal Beam Separations (m)	
(m)	2 beams	8 beams	(m)	2 beams	4, 8 beams
200	*2.02E+04*	*8.09E+04*	*36*	*120 to 161*	*120 to 227*
116	6.36E+03	2.55E+04	20	67 to 90	67 to 127
85	3.48E+03	1.39E+04	15	50 to 67	50 to 94
67	2.04E+03	8.14E+03	11	38 to 51	38 to 72
54	1.46E+03	5.84E+03	10	32 to 43	32 to 61

RESULTS OF THE LIDAR FIXED STARE AND SONIC ANEMOMETER INTER-COMPARISON

In the LIDAR fixed stare and sonic anemometer inter-comparison, data was collected for a total of 2.75 hours over the course of five nights and after removing unusable LIDAR records, 2 hours of data remained. All but about 10 minutes of the usable data was taken at the 116-m level. Wind speeds in the corresponding sonic records ranged between 6 and 15 m/s, but due to varying degrees of misalignment between the LIDAR orientation and the mean wind direction, the streamwise LIDAR velocities ranged between approximately 0 and 12 m/s.

In order to account for the LIDAR's occasionally large misalignment with the wind direction, the total wind vector from the sonic anemometer was projected onto a vector aligned in the direction of the LIDAR beam's orientation. The contents of Table 2 summarize the inter-comparisons of these records using both unsmoothed data and data smoothed using a 1-minute running average filter. The mean difference shown in the table indicates that the LIDAR measurements were on average 0.14 m/s higher than the projected sonic wind speeds. Taking the rate of change of wind speed with height into account in the LIDAR measurements rather than assuming a linear rate by averaging Range Gates 6 and 7 made only a negligible difference in these results.

Table 2. Inter-Comparison of Wind Speeds Measured by LIDAR and Sonic Anemometers

	Mean Difference (m/s)	RMS of Difference (m/s)	Mean Standard Deviation of Difference (m/s)	Median Cross-Correlation Coefficient
Unsmoothed	0.14	0.44	0.30	0.77
One-Minute Smoothed	0.14	0.34	0.12	0.95

A Comparison with Previous Measurements

The results of a similar experiment in 1984 were reported by Hall, et al [9] which employed a CO_2 infrared laser predecessor of the present HRDL and a similar sonic anemometer. In this experiment both a 3-axis sonic and a propeller-vane anemometer were placed atop the NOAA 300-m Boulder Atmospheric Observatory (BAO) Tower near Erie, CO. The winds were measured 1.5 km from the tower (about the minimum range for that LIDAR) and 300 m above the ground. A total of 308 independent radial velocity measurements were made by the LIDAR using a conical scanning mode that took 40 s to make one complete 360º revolution. A velocity-azimuth-diagram or VAD was fitted to the resulting sinusoid of mean wind speed with azimuth angle to determine the wind speed and direction. A total of twenty-five cases were obtained over a wind speed range of less than 1 to more than 20 m/s. The RMS wind speed difference between the velocities measured by the LIDAR and the BAO sonic anemometer for these cases was 0.34 m/s. In Table 3 we compare the BAO results with those from our Lamar experiment. Like the BAO experiment, we inter-compared the *mean differences* found from each of the individual records. Calculated this way, the RMS variation of the mean differences is 0.31 m/s over nominal record lengths of 10 minutes. As can be seen from Table 3, this value compares very favorably with the BAO Tower results [9] at least in terms of the random variation.

Table 3. Inter-Comparison of Mean Differences Between Wind Speeds Measured by Pulsed LIDARs and Sonic Anemometers

	Mean Bias (m/s)	Standard Deviation of Mean Differences (m/s)	RMS of Mean Differences (m/s)
Lamar	0.14	0.27	0.31
BAO Tower[9]	N/A	N/A	0.34

## Sonic Anemometers, SODAR, and LIDAR Vertical Scan-Mode Inter-comparison Results

The results above compared the measured means over a number of observed records and operating conditions in terms of a mean bias or offset and the magnitude of the observed random error. Ideally the correlation between the measured mean wind speeds derived from the sonic anemometer and the LIDAR

should be one, i.e., there is no wind speed dependence, and the mean difference between them should be zero. A numerical method to evaluate this relationship is to compute a linear regression of the corresponding pairs of mean wind speeds measured by the LIDAR and sonic anemometers. A perfect fit would have a slope of unity and a zero offset or bias. Deviations from one in the slope indicate the degree to which the relationship between the two measured wind speeds is itself a function of wind speed. A non-zero offset or bias indicates a fundamental difference exists as a function of wind speed. We now summarize the results of the inter-comparison between the tower-mounted sonic anemometers, the equivalent heights measured by the SODAR, and the vertical-scan mode of the HRDL.

The observed relationship of the observed SODAR values of mean U_H with the corresponding values from all four of the sonic anemometers on the tower are shown in Figure 18. We have calculated the linear regression for the two mean wind speeds which is plotted in the figure. While the bias is low (+0.12 m/s with the sonics reading higher than the SODAR), there is a definite increase in the wind speed difference with increasing wind speed. This not surprising given the level of flow distortion affecting the sonic anemometer measurements discussed previously. The relationship between the mean values of U_H determined from the LIDAR vertical-scan mode and the sonic anemometers is plotted in Figure 19. The corresponding linear regression line shows that there is a large and distinct bias between these two measuring systems of −1.02 m/s with the LIDAR reading lower than the sonics. Finally, Figure 20 shows the relationship of U_H between the vertical-scan mode LIDAR and the SODAR. In this case there is even a larger bias
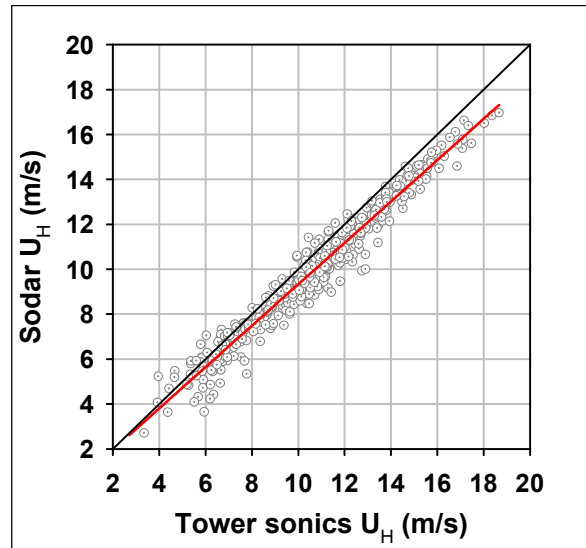
Figure 18. Observed variation and linear regression fit of SODAR U_H versus sonic U_H at all four heights.
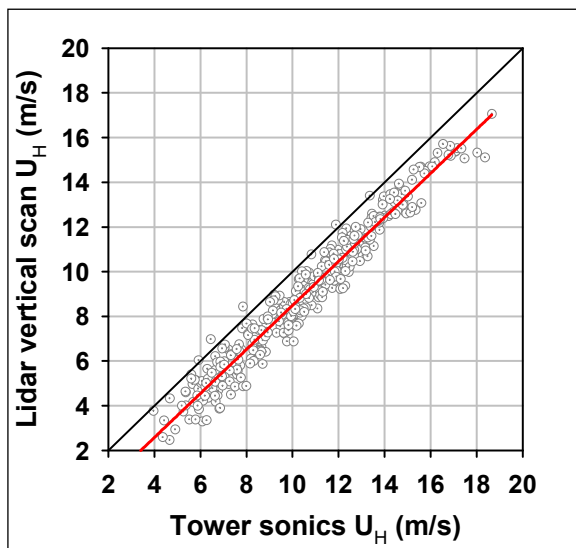
Figure 19. Observed variation and linear regression fit of vertically-scanned mode U_H versus sonic U_H at all four heights.
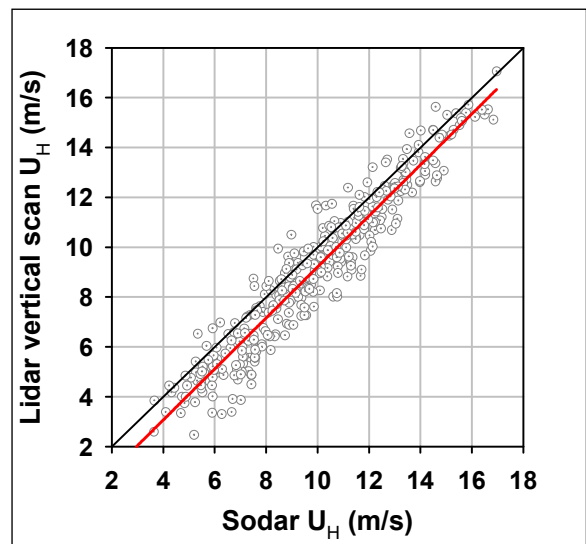
Figure 20. Observed variation and linear regression fit of vertically-scanned mode U_H versus SODAR U_H at the equivalents of all four of the sonic anemometer heights.

(−1.35 m/s) between the LIDAR and SODAR observations. Table 4 summarizes the linear regression results of these inter-comparisons where R^2 is the regression coefficient of determination.

Table 4. Linear Regression Results for the Lamar Inter-Comparison of U_H from Sonics, SODAR, and LIDAR Vertical-Scan Mode

Regression Parameter	SODAR vs Sonics	LIDAR vs Sonics	LIDAR vs SODAR
Bias (m/s)	+0.12 ± 0.11	−1.02 ± 0.16	−1.35 ± 0.12
Slope	0.921 ± 0.010	1.023 ± 0.010	0.984 ± 0.011
Standard Deviation (m/s)	0.65	0.89	0.67
R^2	0.956	0.918	0.955

From Table 4 we see that the observed deviations of UH between the pairs of measurement systems all vary linearly with wind speed, the largest of which are associated with the SODAR and sonic anemometers. This can largely be explained by the influence of the flow distortion seen around the sonic anemometers shown in Figures 9 and 10. The slopes related to the UH differences seen between the LIDAR and the sonics and between the LIDAR and the SODAR exhibit a much smaller variation with wind speed but also reverse in sign about the same speed. We believe the negative large biases observed in the inter-comparisons of the LIDAR and sonics and the LIDAR and SODAR are largely a consequence of the vertical binning technique used to obtain the wind profiles from the LIDAR vertical-scan mode for the reasons stated previously; i.e., a lack of horizontal homogeneity and spatial sampling errors.

Comparison of Lamar Results with those from BAO Experiment

We computed linear regressions of the variation of the differences in LIDAR-derived radial wind speeds using the stare mode with from the sonic anemometers from the BAO [9] and Lamar experiments. The results are plotted in Figure 21. The data from both experiments are very similar; i.e., the LIDARs read higher than the sonics below a mean wind speed of 10 m/s and lower above. Table 5 summarizes the nearly identical results of the linear regression analysis of the data from each of the experiments. The BAO and Lamar Towers are both of triangular lattice construction with vertically-tapered cylindrical apex legs. The structural cross members of the BAO Tower consist of T-shaped beams with sharp edges unlike the cylindrical shape used on the Lamar Tower. The porosity of the BAO
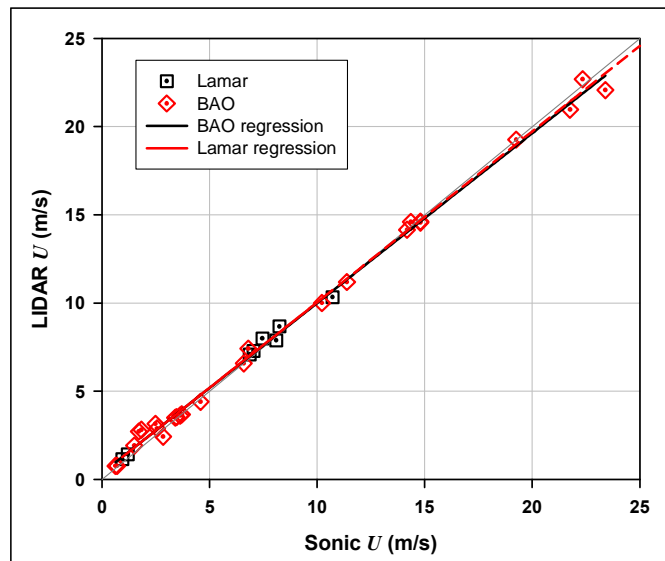
Figure 21. Comparisons and linear regressions of the LIDAR and sonic anemometer wind speeds for the Lamar and BAO tower inter-comparisons. The Lamar regression (black) has been extrapolated beyond its highest value with a dashed line for ease of comparison with the BAO.

17

Table 5. Comparison of Linear Regressions of LIDAR – Sonic Anemometer U_H Differences from the BAO and Lamar Experiments

Regression Parameter	BAO	Lamar
Bias (m/s)	+0.37 ± 0.13	+0.36 ± 0.24
Slope	0.962 ± 0.011	0.966 ± 0.033
Standard Deviation (m/s)	0.50	0.31
R^2	0.997	0.992

Tower appears to be somewhat greater than its Lamar counterpart due to the number of electrical conduits installed on the sides and the elevator shaft within the structure. The Lamar sonic anemometers were mounted more than 5 m away from the tower envelope while the BAO sonic was installed on the top of the 300-m tower where the dimensions are much smaller than at the base. Like the Lamar Tower, we believe the flow distortion pattern around the upper portion and top of the BAO Tower is heavily influenced by Reynolds number effects on the large, cylindrical apex legs.   There is no mean difference in wind speed between the LIDAR and sonic anemometer when the wind speeds are between 10 and 12 m/s as shown in Figure 21. Thus we believe the close agreement shown in Table 5 is a consequence of similar flow distortion patterns likely occurring on both towers in the vicinity of the sonic anemometers.

LONG-TERM INTER-COMPARISON OF SODAR AND TOWER SONIC ANEMOMETERS

 The Scintec SODAR and the tower sonic anemometers were operated in parallel from late May 2002 through mid November 2002 (excluding October 2002) and then again for the two week period in September 2003 when the HRDL LIDAR was on site. During these periods we collected 585 hours of often simultaneous observations of SODAR-derived and sonic anemometer wind speeds and directions. These records were often not contiguous in time because we accepted SODAR horizontal wind vector measurements only when the SODAR return signals exhibited a high or very high SNR and the mean wind direction did not place the tower structure upwind of the sonic anemometers (100 to 140 degrees).   The overall mean U_H difference for the entire available record is −0.13 m/s (with the sonics reading higher) with a random variation or standard deviation of 1.49 m/s. The results are plotted in Figure 22 and the results of the linear regression analysis of the mean U_H differences between the SODAR and the four sonic anemometers are summarized in Table 6. It is clear that there are issues with some of the individual SODAR measurements even with the
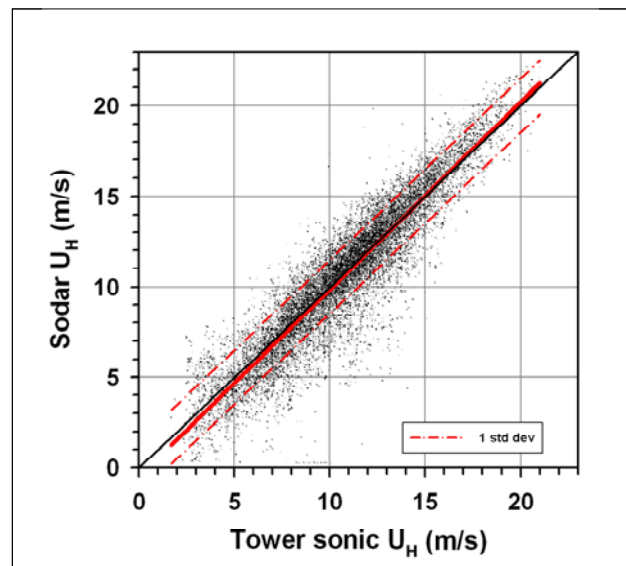
Figure 22. Observed variation and linear regression fit of long-term record of SODAR U_H versus sonic U_H at all four heights.

existence of high and very high SNRs. These are first manifested by the large random variation (standard deviation) in Table 6 compared with Table 4 and then by the relatively large number of individual SODAR readings that occur well below the 1:1 and linear regression lines plotted on Figure 22. The average capture ratio of the number of usable SODAR observations to the number of observations collected during the total time the instrument was in operation is $78 \pm 11\%$ and varies from 64 to 91% for any particular month.

Table 6. Linear Regression Analysis Results of High SNR SODAR – Sonic Anemometers UH Differences for Long-Term Record

Regression Parameter	SODAR – Sonic U_H Difference
Bias (m/s)	-0.50
Slope	1.035
Standard Deviation (m/s)	1.49
R^2	0.845

CONCLUSIONS

Even with instruments mounted more than five tower widths away from the tower structural envelope we found significant levels of flow distortion when the sonic anemometer wind speeds and directions were compared with those measured by the nearby SODAR under high reliability conditions. Typically the wind speed differences were an inverse function of the wind speed which we have attributed to Reynolds number effects in the flow around the cylindrical structural elements. These differences were also found to be a function of the height and wind direction or flow approach angle which is a consequence of the triangular shape of the tower and the location of various mounted equipment. Thus it was clear that the wind speed and directions measured by the tower sonic anemometers, though very accurate themselves, could not be used as the primary reference except in very limited circumstances.

We were able to obtain a reasonable estimate of the expected accuracy of the LIDAR wind speed measurement with respect to the in-situ measurements by employing a scanning mode optimized to minimize the effects of the tower flow distortion on the sonic anemometers. These results agreed very closely with an earlier similar experiment using a 300-m tower and a predecessor of the current HRDL LIDAR. We found that, in the mean, the LIDAR read 0.14 m/s higher than the sonic anemometers with standard deviation of 0.30 m/s with no smoothing applied and 0.12 m/s if smoothed over a period of one minute. The RMS random variation of the mean differences was found to be 0.31 m/s for the Lamar Tower and 0.34 m/s for the earlier experiment using the 300-m tower.

Our inter-comparisons of the horizontal wind speed differences between the sonic anemometers, SODAR, and LIDAR found that the differences generally were a function of the wind speed. The majority of the LIDAR-measured wind speed profiles were derived using a vertical-scan mode and the application of a vertical binning technique. When comparing the LIDAR with the sonics and the LIDAR with the SODAR using this technique we found in the mean the LIDAR read much lower; i.e., -1.02 ± 0.16 m/s compared with the sonics and -1.35 ± 0.12 m/s against the SODAR. We have attributed these larger differences to a combination of the flow distortion around the tower and limitations in the vertical binning

methodology. We found that the magnitude of the wind speed differences, while still a function of the wind speed, were smaller (~ ± 2.5%) than when comparing the SODAR with the tower sonic anemometers (~ −8%).

A long-term inter-comparison of the SODAR-derived horizontal mean wind speeds with the corresponding tower sonic anemometer measurements was available for 585 hours of SODAR operation over a several month period and a wide range of wind directions and speeds. Only high or very high confidence (SNR) SODAR data was used for this comparison. Over the entire available record, the mean difference between the SODAR and the sonic anemometers was −0.13 m/s (sonics higher) with a random variation (standard deviation) of 1.49 m/s. Even with high SNR levels, there were a significant number of instances where the SODAR was indicating mean wind speeds well below and occasionally above those being measured by the sonic anemometers at moderate and higher wind speeds and which contribute to the rather large random variation.

This exercise has demonstrated that both SODARs and LIDARs are capable of making accurate wind speed measurements when atmospheric conditions are favorable and the received signals are processed properly, and in the case of the pulsed LIDAR, an optimum scanning mode is used. It also has been demonstrated that great care must be taken when comparing remote sensing measurements with tower-based measurements.

ACKNOWLEDGEMENTS

REFERENCES

1. Kelley, N.D. (March 2004). "An Initial Overview of Turbulence Conditions Seen at Higher Elevations over the Western Great Plains," *Global Windpower 2004 Conference Proceedings* (CD-ROM), 28-31 March 2004, Chicago, Illinois. Washington, DC: American Wind Energy Association; Omni Press; 12 pp.; NREL Report No. CP-500-35970.

2. Kelley, N.; Shirazi, M.; Jager, D.; Wilde, S.; Adams, J.; Buhl, M.; Sullivan, P.; Patton, E. (2004) *Lamar Low-Level Jet Program − Interim Report*. National Renewable Energy Laboratory. Golden, CO. NREL Report TP-500-34593. 216 pp.

3. Grund, C.J.; Banta, R.M.; George, J.L.; Howell, J.N.; Post, M.J.; Richter, R.A.; Weickman, A.M. (March 2001). "High-Resolution Doppler Lidar for Boundary Layer and Cloud Research," *J. Atmospheric & Oceanic Technology* (18), pp.376-393.

4. Kelley, N. D.; Jonkman, B. J.; Bialasiewicz, J. T.; Scott, G. N.; Redmond, L. S. (2005). "Impact of Coherent Turbulence on Wind Turbine Aeroelastic Response and its Simulation." *Windpower 2005 Conference Proceedings* (CD-ROM), 15-18 May 2005, Denver, Colorado. Washington, DC: American Wind Energy Association; Content Management Corp. 22 pp.; NREL Report No. CP-500-40187.

5. Wieselsberger, C. (1923). "Versuche über den Widerstand gerundeter kantiger Körper," *Ergebinisse AVA Göttingen II Lieferung.* (As referenced in Achenbach [7]).

6. Fage, A.; Falkner, V.M. (1931). "Further experiments on the flow around a circular cylinder," *Aero. Research Council London R. & M.,* No. 1369. (As referenced in Achenbach [7]).

7. Achenbach, E. (1968). "Distribution of local pressure and skin friction around a circular cylinder in cross-flow up to $Re = 5x10^6$," *J. Fluid Mech*. (34), Part 4, pp.625-639.

8. Brewer, W.A. (April 26, 2007). *Personal communication.* NOAA/ESRL, Boulder, CO.

9. Hall, F. F.; Huffaker, R.M.; Hardesty, R.M.; Jackson, M.E.; Lawrence, T.R.; Post, M.J.; Richter, R.A.; Weber, B.F. (August 1984). "Wind Measurement Accuracy of the NOAA Pulsed Infrared Doppler Lidar," *Applied Optics* (23), No. 15, pp. 2503-2506.